Annals of Nuclear Medicine Vol. 19, No. 8, 655–659, 2005

Distinct different intra-tumor distribution of FDG between early phase and late phase in mouse fibrosarcoma

Osamu INOUE,* Miho SHUKURI,* Rie HOSOI,* Misato AMITANI,*
Nariaki MATSUURA,** Jun HATAZAWA*** and Nobuhiko TAKAI****

*Department of Biomedical Physics and Engineering Laboratory,
and **Department of Molecular Pathology, Course of Allied Health Sciences,
Graduate School of Medicine, Osaka University
***Department of Nuclear Medicine and Tracer Kinetics, Graduate School of Medicine, Osaka University
****Heavy-Ion Radiobiology Research Group, National Institute of Radiological Sciences

An early image of intra-tumor distribution of ^{14}C-labeled fluorodeoxy glucose (^{14}C-FDG) was compared with a late image of ^{18}F-labeled FDG (^{18}F-FDG) using mouse fibrosarcoma. Heterogeneous intra-tumor distribution of ^{14}C-FDG was observed 1 minute post injection of the tracer, whereas relatively homogeneous distribution of ^{18}F-FDG was seen 30 minutes later. ^{14}C-FDG was particularly taken up in the peripheral part of the tumor immediately after the tracer injection. A gradual and significant increase in ^{18}F-FDG accumulation with time was seen in the central part of tumor, which indicated an enhancement of anaerobic glycolysis. An initial uptake of ^{18}F-FDG was also compared with distribution of ^{14}C-iodoantipyrine and ^{14}C-thymidine uptake. Intratumoral distribution of initial uptake of ^{18}F-FDG showed almost the same regional distribution of ^{14}C-iodoantipyrine. A similar distribution of ^{14}C-thymidine as the initial uptake of ^{18}F-FDG was also observed. These results indicated that a high initial FDG uptake area seemed to be highly proliferative. A significant difference in the intratumoral distribution of FDG between early phase and late phase seemed to be related to heterogeneous biological characteristics of tumor cells.

Key words: FDG, dual autoradiography, tumor, thymidine, distribution

INTRODUCTION

^{18}F-fluorodeoxy glucose (^{18}F-FDG) has been widely used for detection, staging and monitoring of therapy of various kinds of tumor.[1–3] ^{18}F-FDG uptake has been reported to correlate with tumor proliferation rates in lymphomas and head and neck cancers.[4,5] ^{18}F-FDG uptake is also a useful mean for grading gliomas, breast cancer, lung cancer, pancreatic cancer and sarcomas.[6–10] ^{18}F-FDG uptake in tumor is dependent upon two processes, the delivery process from plasma to tumor and the intratumoral phosphorylation process of FDG to FDG-6-phosphate.[11] The former process is dependent upon regional blood flow and expression of glucose transporters. Hexokinase, a rate-limiting enzyme of glycolysis, is a key enzyme in the latter process. Tumor cells appear to upregulate glucose transporters and increase some of the enzymes associated with metabolic pathways of glucose with increasing malignant transformation.[12–15] With regard to the intratumoral distribution of ^{18}F-FDG, several experimental studies have been reported. A positive correlation between glucose transporter-1 expression and FDG uptake in breast carcinoma was seen.[16] Kubota et al. also reported a positive correlation between ^{18}F-FDG uptake and ^{18}F-fluoromisonidazole, a hypoxia tracer, uptake in AH109A tumor.[17] However, most of the studies on the intratumoral distribution of FDG have been performed using FDG uptake 30 minutes or 60 minutes post tracer injection. As far as we know, there is no report on a direct comparison of the intratumoral distribution of FDG uptake between early phase and late phase after tracer administration, although several dynamic PET studies

Received May 23, 2005, revision accepted August 10, 2005.
For reprint contact: Osamu Inoue, Ph.D., Course of Allied Health Sciences, Graduate School of Medicine, Osaka University, 1–7 Yamadaoka, Suita, Osaka 565–0871, JAPAN.
E-mail: inoue@sahs.med.osaka-u.ac.jp

have been reported.[18,19] In this study, we performed dual tracer autoradiography using ^{18}F-FDG and ^{14}C-FDG on the intratumoral distribution of FDG in the early and late phase. The time points (1 minute for early phase and 30 minutes for late phase) were determined by the time activity data of ^{18}F-FDG in mouse fibrosarcoma as previously reported.[20] A distinct different regional distribution of FDG between the early and late phase was observed. The intratumoral distribution of the early phase of FDG was compared with that of ^{14}C-iodoantipyrine or ^{14}C-thymidine.

MATERIALS AND METHODS

Male C3H mice (12–13 weeks old) were purchased from SLC (Hamamatsu, Japan), and housed at 23–25°C of room temperature in a 12 hours light-dark cycle with free access to food and water. All experiments on the mice were performed with the permission of the Institutional Animal Care and Use Committee, School of Allied Health Sciences, Osaka University. Mice were transplanted with fibrosarcoma (NFSa), and then tracer experiments were performed when the tumor size had reached about 10 mm.

^{18}F-2-fluoro-2-deoxyglucose (^{18}F-FDG) was synthesized with an automated ^{18}F-FDG synthesis system (Sumitomo Heavy Industries, Japan). ^{14}C-2-fluoro-2-deoxyglucose (^{14}C-FDG) was purchased from American Radiolabeled Chemicals Inc. (St. Louis, MO, USA), ^{14}C-iodoantipyrine and ^{14}C-thymidine were from Perkin Elmer Life Science Inc. (Boston, MA, USA).

Mice were intravenously injected with ^{18}F-FDG (740 kBq), and ^{14}C-FDG (37 kBq) was injected at 29 minutes post injection of ^{18}F-FDG. Mice were decapitated at 1 minute after the injection of ^{14}C-FDG, and the tumor was quickly removed and frozen with hexan-dryice. Sections (20 μm) were prepared with a cryostat, and exposed to an imaging plate (Fuji Photo Film, Japan) for 2–4 hours to obtain ^{18}F-FDG images. After the decay of ^{18}F (1–2 days), the sections were re-exposed to an imaging plate for 7–10 days to obtain ^{14}C-FDG images. Regions of interest (ROIs) were made on images, and the radioactivity concentration in each ROI was expressed as the photo stimulated luminescence (PSL) value per mm^2. The data were corrected with radioactivity concentration in the whole tumor (% injected dose/g tissue) determined by tissue dissection method performed in another experiment. The dissected tumors were weighed and counted with a well scintillation counter for ^{18}F or a liquid scintillation counter for ^{14}C. Viability was demonstrated by histological examination after staining with hematoxylin and eosin (H&E).

Dual autoradiograms of ^{18}F-FDG (1 minute post injection) and ^{14}C-iodoantipyrine (1 min post injection), or ^{18}F-FDG (1 minute post injection) and ^{14}C-thymidine (30 minutes post injection) in the same section were also made by the same method as described above. There were 3–4 mice per group in both the autoradiographic study and dissection experiment. The student's t-test was employed for statistical analysis.

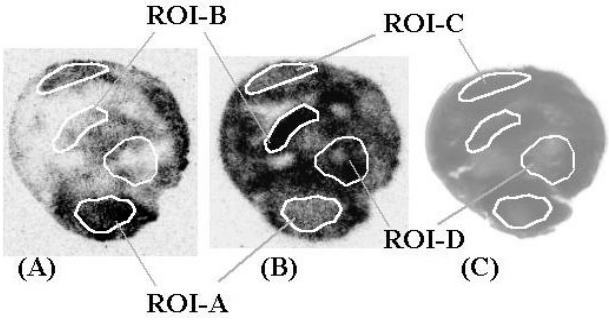

Fig. 1 Intratumoral distribution of ^{14}C-FDG (1 minute after the injection) (A), ^{18}F-FDG (30 minutes after the injections) (B) in the same section of fibrosarcoma. H&E staining (C) shows that most of the tumor cells are viable. Three mice were used in each group.

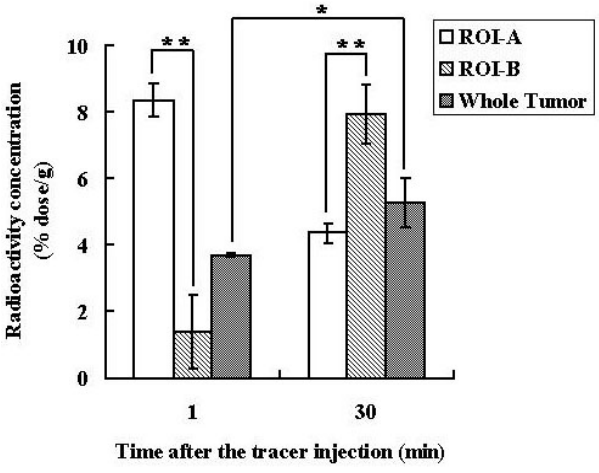

Fig. 2 Radioactivity concentration of labeled FDG in the peripheral area (ROI-A), control area (ROI-B) and the whole-tumor at 1 minute or 30 minutes after the injection of tracers. Radioactivity concentrations of either ^{14}C-FDG or ^{18}F-FDG in whole tumor were determined by the tissue dissection method in another experiment, and values were expressed as percent injected dose per gram tissue (% dose/g). The photo-stimulated luminescence (PSL/mm^2) values in each ROI were corrected by the radioactivity concentration in the whole tumor determined. Average ± SD of three mice in each group. *: $p < 0.05$, **: $p < 0.01$

RESULTS

Figure 1 shows early and late images of the intratumoral distribution of FDG and H&E staining in the same section. Heterogeneous intratumoral distribution of ^{14}C-FDG was observed at 1 minute post injection of the tracer. In an

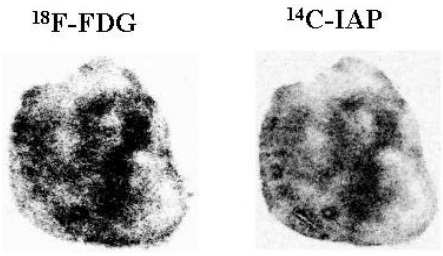

Fig. 3 The regional distribution of ^{18}F-FDG (1 minute post injection) and ^{14}C-iodoantipyrine (1 minute post injection) in the same section of a fibrosarcoma. Four mice were used in each group.

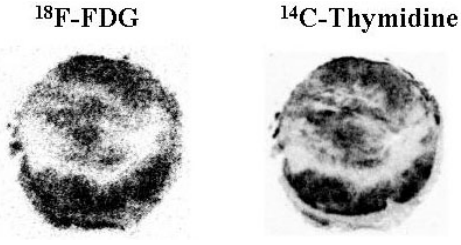

Fig. 4 The regional distribution of ^{18}F-FDG (1 minute post injection) and ^{14}C-thymidine (30 minutes post injection) in the same section of a fibrosarcoma. Four mice were used in each group.

early image, ^{14}C-FDG was particularly distributed in the peripheral area of the fibrosarcoma, and radioactivity concentration in the central part of tumor was very low. In contrast, ^{18}F-FDG was highly accumulated in some parts of the central area although the intratumoral distribution was still heterogeneous. The H&E staining showed that most of the tumor cells were viable as shown in Figure 1-C. In a late image, ^{18}F-FDG uptake in ROI-C (most tumor cells were in a viable area) was lower than that in ROI-D, where necrosis was partly seen in H&E staining. Thus, ^{18}F-FDG uptake in late phase was not directly related to tumor cell viability. Radioactivity concentrations in whole tumor determined by the dissection method were 3.70 ± 0.86% dose/g at 1 minute post injection and 5.26 ± 0.86% dose/g at 30 minutes after the tracer injection. The corrected PSL/mm^2 value in each ROI using the above radioactivity concentrations in whole tumor is shown in Figure 2. In the peripheral area (ROI-A), accumulation of FDG decreased to about half of the initial uptake during 30 minutes post injection. In contrast, a pronounced increase in the accumulation of FDG was observed in the central part of the tumor (ROI-B). The regional distribution pattern of initial uptake of FDG in fibrosarcoma was similar to that of ^{14}C-iodoantipyrine (Fig. 3). A similar intratumoral distribution of ^{18}F-FDG as regional uptake of ^{14}C-thymidine was also observed as shown in Figure 4.

DISCUSSION

The initial regional uptake of labeled FDG in fibrosarcoma was quite different from the intratumoral distribution of FDG observed at 30 minutes post injection. The uptake of FDG was mainly dependent upon two processes, the plasma-tumor delivery process and phosphorylation of FDG by hexokinase.[11] An early phase of FDG uptake into tumor might reflect the delivery process from the plasma; therefore the regional blood flow and glucose transporter may play crucial roles in the initial uptake of FDG. In addition, the effects of blood volume and interstitial space upon the initial distribution of FDG should be considered. Tumor blood volume of in a C3H mouse mammary carcinoma estimated by T1-weighted dynamic contrast enhanced-magnetic resonance imaging (DCE-MRI) was reported to be about 7%.[21] Taken together with the fact that ^{18}F-FDG concentration in plasma 1 minute post injection was about 8% dose/g,[20] the effect of blood volume on FDG uptake in tumor seemed to be not so large. The effect of interstitial space on the initial uptake of FDG is not known yet, and further study is needed. In this study, intratumoral distribution of ^{18}F-FDG 1 minute post injection was similar to that of ^{14}C-iodoantipyrine as shown in Figure 3. In the area, in which high initial uptake of FDG was seen, the blood supply seemed to be sufficient for oxidative glucose metabolism in tumor cells. The measurement of blood flow, blood volume and integrity of tumor microvessels is important to understand tumor growth and to evaluate the response to therapy.[22,23] Tozer et al. reported an approximately 100-fold decrease in tumor blood flow 6 hours after the treatment with disodium combretastatin A-4 3-*O*-phosphate (CA-4-P), a tumor vascular-targeting agent, using the ^{14}C-iodoantipyrine method.[24] It would, therefore, be of interest to know whether the initial uptake of FDG is also decreased by treatment with CA-4-P.

In contrast, the rate of phosphorylation of FDG by HK in the tumor might play a critical role in the accumulation of FDG during the 30 minutes after the tracer injection. In the central part of the tumor (ROI-B), a significant increase in HK activity was indicated as compared with the peripheral area of tumor (ROI-A). As shown in Figure 2, the radioactivity concentration in ROI-B at 30 minutes after the tracer injection was more than 3-fold that at 1 minute post injection, whereas the radioactivity concentration in ROI-A decreased with time after the tracer injection. Anaerobic glycolysis might be enhanced in the central part of tumor (ROI-B), and this area seemed to be relatively hypoxic due to a poor blood supply. The early images of FDG mainly reflect the delivery process, and the late images reflect both delivery and phosphorylation processes. The subtraction of the early image of intratumoral FDG distribution from the late image might be of some value to assess the phosphorylation process in tumor, which might be related to a relatively intratumoral

hypoxic region. Hypoxia induces an aggressive phenotype, increasing metastatic potential, promoting tumor progression, and limiting the effectiveness of radiation therapy.[25,26] Successful imaging of hypoxia has been performed using ^{14}C-misonidazol.[27] The comparison of the regional distribution of the early phase of ^{14}C-FDG and ^{18}F-misonidazol would make an interesting subject for a future study.

The early distribution of ^{18}F-FDG was almost the same as the intratumoral distribution of ^{14}C-thymidine. The tumor areas, in which FDG had highly accumulated at 1 minute post injection, were found to be proliferative. It has been well documented that tumor growth is associated with vigorous neoangiogenesis. The current study revealed that the highly proliferative areas, in which a high initial uptake of FDG was seen, corresponded to the same areas with a high blood supply. These observations suggested the importance of regional kinetic analysis of ^{18}F-FDG in tumor, despite a limitation of spatial resolution either human or animal PET cameras. To clarify the relationship between kinetic changes in intratumoral distribution of FDG and biological properties of tumor cells is an important subject for future study.

REFERENCES

1. Wahl RL, Cody RL, Hutchins GD, Mudgett EE. Primary and metastatic breast carcinoma: initial clinical evaluation with PET with the radiolabeled glucose analogue 2-[F-18]-fluoro-2-deoxy-D-glucose. *Radiology* 1991; 179: 765–770.
2. Delbeke D. Oncological applications of FDG PET imaging: brain tumors, colorectal cancer, lymphoma and melanoma. *J Nucl Med* 1999; 40: 591–603.
3. Ak I, Stokkel MP, Pauwels EK. Positron emission tomography with 2-[^{18}F]fluoro-2-deoxy-D-glucose in oncology. Part II. The clinical value in detecting and staging primary tumors. *J Cancer Res Clin Oncol* 2000; 126: 560–574.
4. Okada J, Yoshikawa K, Itami M, Imaseki K, Uno K, Itami J, et al. Positron emission tomography using fluorine-18-fluorodeoxyglucose in malignant lymphoma: a comparison with proliferative activity. *J Nucl Med* 1992; 33: 325–329.
5. Smith TAD, Titley J. Deoxyglucose uptake by head and neck squamous carcinoma: Influence of change in proliferative fraction. *Int J Radiat Oncol Biol Phys* 2000; 47: 219–223.
6. Di Chiro G, DeLaPaz RL, Brooks RA, Sokoloff L, Kornblith PL, Smith BH, et al. Glucose utilization of cerebral gliomas measured by [^{18}F]fluorodeoxyglucose and positron emission tomography. *Neurology* 1982; 32: 1323–1329.
7. Nieweg OE, Kim EE, Wong WH, Broussard WF, Singletary SE, Hortobagyi GN, et al. Positron emission tomography with fluorine-18-deoxyglucose in the detection and staging of breast cancer. *Cancer* 1993; 71: 3920–3925.
8. Vesselle H, Schmidt RA, Pugsley JM, et al. Lung cancer proliferation correlates with [F-18]fluorodeoxyglucose uptake by positron emission tomography. *Clin Cancer Res* 2000; 6: 3837–3844.
9. Nakata B, Chung YS, Nishimura S, Nishihara T, Sakurai Y, Sawada T, et al. ^{18}F-fluorodeoxyglucose positron emission tomography and the prognosis of patients with pancreatic adenocarcinoma. *Cancer* 1997; 79: 695–699.
10. Folpe AL, Lyles RH, Sprouse JT, Conrad EU 3rd, Eary JF. (F-18) fluorodeoxyglucose positron emission tomography as a predictor of pathologic grade and other prognostic variables in bone, and soft tissue sarcoma. *Clin Cancer Res* 2000; 6: 1279–1287.
11. Pauwels EK, Sturm EJ, Bombardieri E, Cleton FJ, Stokkel MP. Positron-emission tomography with [^{18}F]fluorodeoxyglucose. Part I. Biochemical uptake mechanism and its implication for clinical studies. *J Cancer Res Clin Oncol* 2000; 126: 549–559.
12. Smith TA. Facilitative glucose transporter expression in human cancer tissue. *Br J Biomed Sci* 1999; 56: 285–292.
13. Reisser C, Eichhorn K, Herold-Mende C, Born AI, Bannasch P. Expression of facilitative glucose transport proteins during development of squamous cell carcinomas of the head and neck. *Int J Cancer* 1999; 80: 194–198.
14. Arora KK, Pedersen PL. Functional significance of mitochondrial bound hexokinase in tumor cell metabolism. Evidence for preferential phosphorylation of glucose by intramitochondrially generated ATP. *J Biol Chem* 1988; 263: 17422–17428.
15. Smith TA. Mammalian hexokinases and their abnormal expression in cancer. *Br J Biomed Sci* 2000; 57: 170–178.
16. Brown RS, Leung JY, Fisher SJ, Frey KA, Ethier SP, Wahl RL. Intratumoral distribution of tritiated-FDG in breast carcinoma: correlation between Glut-1 expression and FDG uptake. *J Nucl Med* 1996; 37: 1042–1047.
17. Kubota K, Tada M, Yamada S, Hori K, Saito A, Iwata R, et al. Comparison of the distribution of fluorine-18 fluoromisonidazole, deoxyglucose and methionine in tumour tissue. *Eur J Nucl Med* 1999; 26: 750–757.
18. Gupta N, Gill H, Graeber G, Bishop H, Hurst J, Stephens T. Dynamic positron emission tomography with F-18 fluorodeoxyglucose imaging in differentiation of benign from malignant lung/mediastinal lesions. *Chest* 1998; 114: 1105–1111.
19. Torizuka T, Nobezawa S, Momiki S, Kasamatsu N, Kanno T, Yoshikawa E, et al. Short dynamic FDG-PET imaging protocol for patients with lung cancer. *Eur J Nucl Med* 2000; 27: 1538–1542.
20. Kobayashi K, Hosoi R, Momosaki S, Koike S, Ando K, Nishimura T, et al. Enhancement of the relative uptake of ^{18}F-FDG in mouse fibrosarcoma by rolipram. *Ann Nucl Med* 2002; 16: 507–510.
21. Bentzen L, Vestergaard-Poulsen P, Nielsen T, Overgaard J, Bjornerud A, Briley-Saebo K, et al. Intravascular contrast agent-enhanced MRI measuring contrast clearance and tumor blood volume and the effects of vascular modifiers in an experimental tumor. *Int J Radiat Oncol Biol Phys* 2005; 61: 1208–1215.
22. Ostergaard L, Hochberg FH, Rabinov JD, Sorensen AG, Lev M, Kim L, et al. Early changes measured by magnetic resonance imaging in cerebral blood flow, blood volume, and blood-brain barrier permeability following dexamethasone treatment in patients with brain tumors. *J Neurosurg* 1999; 90: 300–305.
23. Miller JC, Pien HH, Sahani D, Sorensen AG, Thrall JH. Imaging angiogenesis: applications and potential for drug

development. *J Natl Cancer Inst* 2005; 97: 172–187.
24. Tozer GM, Prise VE, Wilson J, Locke RJ, Vojnovic B, Stratford MR, et al. Combretastatin A-4 phosphate as a tumor vascular-targeting agent: early effects in tumors and normal tissues. *Cancer Res* 1999; 59: 1626–1634.
25. Young SD, Marshall RS, Hill RP. Hypoxia induces DNA over replication and enhances metastatic potential of murine tumor cells. *Proc Natl Acad Sci USA* 1988; 85: 9533–9537.
26. Brown MJ. The hypoxic cell: a target for selective cancer therapy. *Cancer Res* 1999; 59: 5863–5870.
27. Chapman JD, Franko AJ, Sharplin J. A marker for hypoxic cells in tumours with potential clinical applicability. *Br J Cancer* 1981; 43: 546–550.